Monosynaptic tracing success depends critically on helper virus concentrations

Thomas K. Lavin[1], Lei Jin[1], Nicholas E. Lea[1] & Ian R. Wickersham[1]

[1]McGovern Institute for Brain Research, Massachusetts Institute of Technology, Cambridge, MA 02139, USA

ABSTRACT

Monosynaptically-restricted transsynaptic tracing using deletion-mutant rabies virus has become a widely used technique in neuroscience, allowing identification, imaging, and manipulation of neurons directly presynaptic to a starting neuronal population. Its most common implementation is to use Cre mouse lines in combination with Cre-dependent "helper" adeno-associated viral vectors (AAVs) to supply the required genes to the targeted population before subsequent injection of a first-generation (ΔG) rabies viral vector. Here we show that the efficiency of transsynaptic spread and the degree of nonspecific labeling in wild-type control animals depend strongly on the concentrations of these helper AAVs. Our results suggest practical guidelines for achieving good results.

INTRODUCTION

Rabies virus has proven useful for neuroscience, because of its natural behavior of spreading between synaptically-connected neurons (although both the mechanism of transsynaptic spread and the true degree of its synaptic specificity remain unclear[1; 2]) in an apparently exclusively retrograde direction (in the central nervous system, whereas in primary sensory neurons it appears to be bidirectional[3; 4]). This has allowed it to serve as a useful tool for mapping synaptic connections, usually in the context of "monosynaptic tracing", which refers to the use of a modified rabies virus to label neurons that are, putatively, directly presynaptic to a targeted population of neurons[5]. It relies on the use of a rabies virus to which two modifications have been made. First, in order to render it incapable of spread between neurons without assistance, one (or more) of its genes has been deleted; in first-generation vectors, this is the glycoprotein gene, denoted "G"[6]. Second, in order to allow selective targeting of the initial infection to the group of neurons of interest, the viral particles are coated with the envelope protein of a different virus (the avian-endemic retrovirus "ASLV-A"; the envelope protein of which is called "EnvA"), rendering the virus incapable of infecting mammalian neurons without assistance[5]. In the targeted neuronal population, two exogenous proteins must be expressed before injection of the rabies virus: the receptor for EnvA (a quail cell surface protein called "TVA"[7]), to allow the modified rabies virus to infect the starting cells, and the deleted viral gene(s) (G, in the case of first-generation ("ΔG") vectors). While this can be achieved by single-cell transfection techniques[8; 9; 10; 11], the much more accessible and widely used implementation is to use Cre[12]-dependent adeno-associated viral vectors ("AAVs")[13; 14; 15; 16; 17; 18; 19; 20; 21] in combination with a Cre mouse line, in order to map inputs to a Cre-expressing group of neurons (see Figure 1). This approach has been used in a large number of studies and (if we may say so) contributed considerably to our understanding of the organization of many circuits within the mammalian nervous system.

Within this basic paradigm of using Cre-dependent "helper" AAVs to provide the genes required for monosynaptic tracing, many variations are possible. A major consideration in design of such experiments is the mismatch between the miniscule amount of TVA required for successful initial infection of the starting cells, because of the high sensitivity of the EnvA-TVA interaction[22; 23], and the high levels of G that appear to be required for efficient spread of the virus from the starting cells to the putatively presynaptic cells. This causes a problem: to achieve acceptable levels of transsynaptic spread, a high concentration of AAV may be found to be necessary; however, because it appears that all putatively Cre-dependent AAVs "leak" because of spontaneous recombination of some fraction of virions' genomes, even at the plasmid DNA stage (unpublished results and Kim Ritola, personal communication), a high concentration of an AAV expressing TVA can result in an unacceptably high level of "background" labeling of cells by the rabies virus in wild-type mice. Different groups have taken different approaches to dealing with this, including using two separate Cre-dependent AAVs so that G is expressed at a presumably higher level than TVA[15] and/or using a low-affinity mutant of TVA[24; 25].

Our current approach is to use a mixture of two AAVs, described first in Liu et al.[18], which are coupled by the tetracycline transactivator system[26]. The first AAV is Cre-dependent and expresses, in Cre-expressing cells, TVA (transmembrane isoform[7; 27; 28]), EGFP[29], and the tetracycline transactivator ("tTA"); the second is not directly Cre-dependent but simply expresses both G (SAD B19 strain[30]) and the blue fluorophore mTagBFP2[31] under the control of the tetracycline response element. Expression of tTA from the first AAV

drives expression of G from the second AAV in the same cells. Note that this uses the "TET-OFF" system, so that no tetracycline (or doxycycline, etc.) needs to be added in order to make the system work.

The use of this combination has several intended advantages. First, the use of a two-AAV combination allows the concentrations of the vectors encoding TVA and G to be independently titrated. Second, the tTA-TRE system should provide amplification of the level of G expression with respect to the level of expression of the genes in the first AAV, so that the TVA/EGFP/tTA virus can be titrated down to very low concentration to result in low background labeling in wild-type mice but with the G expression level still high enough to result in plentiful transsynaptic spread of the rabies virus. Third, the use of the tet transactivator system theoretically allows the expression of G (and mTagBFP2) to be turned off (or potentially titrated) by administration of doxycycline after transsynaptic spread has taken place, in order to mitigate toxicity to the starting cells, but we have not done this in any of the work presented in this paper.

We have recently published a detailed step-by-step protocol for monosynaptic tracing using these viruses for monosynaptic tracing with Cre mice [44]. Here we present results of our titration experiments to test the effects of using different dilutions of the helper viruses, to show the reasons for the specific concentrations that we recommend. We found that the two-helper combination described above and in Liu et al.[18] gives much better results than the simpler single AAV which we described earlier[16], which did not allow independent optimization of transsynaptic tracing efficiency and minimization of background labeling in Cre-negative mice. We also found that *excessively high* titers of the helper viruses gave very poor results, suggesting that preventing toxicity due to overly high expression of the helper virus genes is as important as ensuring sufficient expression of them. Finally, and most practically, we suggest specific concentrations of the helper viruses that gave best results in the Cre line in which we performed the titration and that should serve either as a likely choice of parameters for end-users or as a promising starting point for much more limited titration series to be done as pilot experiments when targeting other cell types in other Cre lines.

RESULTS

Having previously found Addgene's Viral Service (www.addgene.org/viral-service/aav-prep) to be an excellent source of high-quality AAVs, we authorized them to package and distribute three of our published Cre-dependent helper AAVs: the standalone helper virus AAV-syn-FLEX-splitTVA-EGFP-B19G from Kohara et al.[16] (referred to below as the "tricistronic" helper virus) and the two viruses to be used in combination as described in Liu et al.[18]: AAV-syn-FLEX-splitTVA-EGFP-tTA and AAV-TREtight-mTagBFP2-B19G. Although the resulting preparations, all with serotype 1 capsids, had much higher titers than earlier batches that we had previously used successfully for similar experiments, we nonetheless first tried using them "straight": undiluted except insofar as, for the two-helper-virus combination, the two viruses were combined in a 50/50 mixture by volume (see Methods). We injected either AAV1-syn-FLEX-splitTVA-EGFP-B19G or the two-virus mixture into the primary somatosensory cortex of either the PV-Cre (expressing Cre from the parvalbumin locus)[32] mouse line crossed with the Ai65F reporter line (FLP-dependent tdTomato[33])[34] or, for Cre-negative controls, the Ai65F reporter line without a Cre allele. 7 days after AAV injection, we injected RVΔG-4FLPo(EnvA)[45] (expressing FLPo recombinase[35]) and perfused the mice 7 days after that.

The results were surprisingly bad. Figure 2, panels a-h show example results using the two-helper combination without dilution. While many cells were well-labeled with EGFP, blue fluorescence was barely visible, and there were few tdTomato-labeled cells at the injection site and almost none elsewhere (see Figure 4 for quantification). Furthermore, matched control injections of the same viruses in Cre-negative mice resulted in undesirably large numbers of RV-labeled neurons at the injection site (Figure 3, panels a-d). This was evidently not the fault of the rabies virus preparation: in control animals injected only with rabies virus, with no helper viruses, we found no RV-labeled cells at the injection site or otherwise (data not shown). While results using the undiluted single tricistronic helper virus looked better in PV-Cre mice, they were still unimpressive, and the problem of label in Cre-negative mice was far worse (see Figure 4 for quantification; example images not shown in these cases).

On the assumption that the poor results in Cre mice were due to toxicity resulting from excessive concentration, we diluted the new preparations to the same titers as those of the batches that we had been using previously: namely, we diluted AAV1-syn-FLEX-splitTVA-EGFP-tTA by a factor of 17.96 (to 9.47 × 10^11 gc/ml, based on the titer reported by Addgene) and AAV1-TREtight-mTagBFP2-B19G by a factor of 19.98 (to 1.60 × 10^12 gc/ml, based on the titer reported by Addgene).

Using these diluted helper viruses gave us much better results, with large numbers of RV-labeled neurons found in upstream regions including secondary somatosensory cortex, thalamus, and contralateral cortex (Figure 2, panels i-p shows example results; see Figure 4 for quantification). However, in mice not expressing Cre, even

using the diluted AAVs resulted in unreasonably-high numbers of RV-labeled neurons (red) (Figure 3, panels e-h, with quantification in Figure 4), as well as bright blue (but no visible green, even with immunostaining) labeling indicative of leaky expression from the helper viruses in the absence of recombinase.

We therefore embarked on a systematic set of experiments testing a range of dilutions for each helper virus, in order to find a set of dilutions for both the two-helper combination and the single helper that would result in efficient transsynaptic label in Cre mice but low background label in Cre-negative mice. For these experiments, the rabies virus used was RV∆G-4mCherry(EnvA)[16], expressing mCherry[33] rather than FLPo. The results of these experiments are quantified in Figure 5, with source numbers given in table S1.

For the two-helper combination (Figure 5, panel a), we were able to find dilutions that resulted in good transsynaptic label in Cre mice with little label at the injection site of Cre-negative mice. We began with 1:20 dilutions of both AAV1-syn-FLEX-splitTVA-EGFP-tTA and AAV1-TREtight-mTagBFP2-B19G, approximating (with simplification) the 1:17.96 & 1:19.98 dilutions used for used for Figures 2-4. Holding the concentration of the TRE AAV constant, we compared dilutions of the FLEX AAV of 1:20, 1:66.67, and 1:200 (labeled in panel a as "0.05x", "0.015x", and "0.005x", respectively). Of these, we found that the most extreme dilution tested, 1:200, worked best, with the numbers of labeled cells in contralateral cortex in Cre mice almost as high as for the 1:20 dilution but with the numbers of labeled cells at the injection site in Cre-negative mice drastically reduced. Holding the concentration of the FLEX AAV constant at 1:200, we then tried increasing the concentration of the TRE AAV, comparing the 1:20 dilution to 1:10 and to undiluted stock. Interestingly, while these two additional conditions resulted in somewhat higher numbers of labeled contralateral cells in PV-Cre mice, they also greatly increased the numbers of cells labeled at the injection site in Cre-negative mice (compare "0.005x tTA & 0.05x TRE" to "0.005x tTA & 1x TRE" in Figure 5, panel a). Because the amount of TVA was not changed across these latter conditions, we assume that the additional labeled cells in Cre-negative mice were due to leaky G expression being sufficient to allow limited transsynaptic spread of the rabies virus from the initially-infected cells.

The best condition tested was therefore AAV1-syn-FLEX-splitTVA-EGFP-tTA 1:200 (for a final titer of 8.5 × 10^10 gc/ml) and AAV1-TREtight-mTagBFP2-B19G 1:20 (for a final titer of 1.6 × 10^12 GC/ml). Example images of results using this combination are shown in Figure 6, panels a-h for Cre mice and Figure 7, panels a-d for Cre-negative mice.

For the single tricistronic helper AAV1-syn-FLEX-splitTVA-EGFP-B19G, we compared undiluted ("1x" in Figure 5 panel b) to 1:3.33, 1:10, and 1:33.3 dilutions ("0.3x", "0.1x", and "0.03x" in the figure). While all the diluted versions improved matters over the undiluted version, none of the dilutions gave particularly good results, with even the highest dilution still resulting in much higher numbers of labeled cells at the injection site in Cre-negative animals than were found with the optimized two-helper combination, but with far fewer transsynaptically labeled cells in Cre mice. Example images of results using the 1:10 dilution are shown in Figure 6, panels i-o for Cre mice and Figure 7, panels e-g for Cre-negative mice.

Finally, to determine whether the dilutions for the two-virus combination that worked best in PV-Cre mice also worked well in another Cre line, we performed a similar experiment in DAT-Cre mice[36], with 1:200 AAV1-syn-FLEX-splitTVA-EGFP-tTA and 1:20 AAV1-TREtight-mTagBFP2-B19G followed by RV∆G-4FLPo(EnvA) a week later. As shown in Figure 8, there were abundant labeled cells in striatum and cortex, suggesting that these helper virus dilutions may work well with other starting cell populations.

DISCUSSION

Our results demonstrate that the success of monosynaptic tracing depends strongly on the complementation strategy (using the two tTA-TRE coupled helper viruses worked much better than the single helper virus expressing TVA, EGFP, and G) and on the concentrations of the helper viruses.

More generally, our findings underscore that monosynaptic tracing results should not be taken as a complete delineation of the set of cells presynaptic to a targeted starting cell group, given that the number of false negatives (unlabeled cells that are actually presynaptic to the starting cells) clearly depends on the experimental parameters.

We have done these titration experiments with cortical injections in PV-Cre or Cre-negative mice. Results with other injection sites and Cre lines will presumably vary depending on the tropism of AAV1 for the targeted cell type and the other cells in the vicinity of the injection site. However, the fact that the parameters that we found to work best in PV-Cre, namely the two-helper combination with dilutions of 1:200 and 1:20, respectively, also gave good results in DAT-Cre mice (Figure 8) may indicate that these could be good general-purpose parameters for most Cre lines; at the very least, they should serve as a good starting point for a much more limited set of titration experiments than we have undertaken here.

METHODS

All experiments involving animals were conducted according to NIH guidelines and approved by the MIT Committee for Animal Care. Mice were housed 1-5per cage under a normal light/dark cycle for all experiments.

Viruses

Cloning of AAV genome plasmids pAAV-synP-FLEX-splitTVA-EGFP-B19G (Addgene 52473), pAAV-syn-FLEX-splitTVA-EGFP-tTA (Addgene 100798), and pAAV-TREtight-mTagBFP2-B19G (Addgene 100799) has been described[16; 18]. These genomes were packaged in serotype 1 AAV capsids by, and are available for purchase from, Addgene (catalog numbers 52473-AAV1, 100798-AAV1, and 100799-AAV1). The titers of the AAVs, as determined by Addgene by qPCR, were as follows:

AAV1-synP-FLEX-splitTVA-EGFP-B19G (lot # v14715): 2.4 × 10^13 gc⁄ml
AAV1-syn-FLEX-splitTVA-EGFP-tTA (lot # v15287): 1.7 × 10^13 gc⁄ml
AAV1-TREtight-mTagBFP2-B19G (lot # v14716): 3.2 × 10^13 gc⁄ml.

Cloning of pRVΔG-4FLPo[45] (Addgene 122050) and pRVΔG-4mCherry[37] (Addgene 52488) have been described. Production of EnvA-enveloped rabies virus RVΔG-4mCherry(EnvA)[16] was done as described previously[38; 39; 40] but using helper plasmids pCAG-B19N (Addgene #59924), pCAG-B19P (Addgene #59925), pCAG-B19G (Addgene #59921), pCAG-B19L (Addgene #59922), and pCAG-T7pol (Addgene #59926) for the rescue step[40]. The final titers were 5.82 × 10^9 infectious units/ml for RVΔG-4FLPo(EnvA) and 1.70 × 10^10 infectious units/ml for RVΔG-4mCherry(EnvA), as determined by infection of TVA-expressing cells as described previously[38][45].

Helper AAVs were diluted in Dulbecco's phosphate-buffered saline (DPBS) (Fisher, 14-190-250) by the desired dilution factors (see main text). In the case of AAV-syn-FLEX-splitTVA-EGFP-tTA and AAV-TREtight-mTagBFP2-B19G, the two viruses were combined (after dilution, when applicable) in a 50/50 ratio by volume before injection.

Mouse strains

Adult mice of both sexes were used. For compatibility with other projects in the laboratory, the PV-Cre (Jackson 017320) and DAT-Cre (Jackson 006660) used were also heterozygous for the FLP-dependent tdTomato reporter line Ai65F[34](obtained in this case by crossing the Cre- and FLP-dependent tdTomato double-reporter line Ai65D[41] (Jackson Laboratory 021875) to the Cre deleter line Meox2-Cre[42] (Jackson Laboratory 003755), then breeding out the Meox2-Cre allele, resulting in a reporter line for which only FLP is required for expression of tdTomato). For those mice in which RVΔG-4FLPo was used, the reporter allele was necessary for reporting RV activity; for those in which RVΔG-4mCherry was used, the presence of this reporter allele was irrelevant. For Cre-negative control injections using RVΔG-4FLPo, the Ai65F line was used. For Cre-negative control injections using RVΔG-4mCherry, either Ai65F or the Cre-dependent reporter line Ai14[43] was used; in these cases, the presence of the reporter alleles was again irrelevant.

Stereotaxic injections

For pilot studies (Figures 2-4), we injected 300 nl of helper AAV solution into primary somatosensory cortex (coordinates with respect to bregma: AP= -0.58 mm, LM = 3.00 mm, DV = -1.00 mm) of anesthetized adult mice as described[44], using a stereotaxic instrument (Stoelting Co., 51925) and custom injection apparatus consisting of a hydraulic manipulator (Narishige, MO-10) with headstage coupled via custom adaptors to a wire plunger advanced through pulled glass capillaries (Drummond, Wiretrol II) back-filled with mineral oil and front-filled with viral vector solution. 7 days after AAV injection, 100 nl of RVΔG-FLPo(EnvA) was injected in the same site.

For subsequent experiments in PV-Cre (Figures 5-7), 200 nl of helper AAV solution was injected, followed by 100 nl of RVΔG-4mCherry(EnvA) 7 days later. For DAT-Cre mice (Figure 8), 200 nl of helper AAV solution was injected (AP= -3.00 mm, LM = 1.50 mm, DV = -4.20 mm), followed by 500 nl of RVΔG-FLPo(EnvA) 7 days later. Two mice were used for each condition (n= 2); for 0.03x sTpEpB, one mouse died prior to perfusion, so data for only one subject are included in Table S1 for that condition.

Perfusions and histology

7 days after injection of rabies virus, mice were transcardially perfused with 4% paraformaldehyde in phosphate-buffered saline. Brains were postfixed in 4% paraformaldehyde overnight on a shaker at 4°C and cut into 50 µm sections on a vibrating microtome (Leica, VT-1000S), with sections collected into six tubes (containing cryoprotectant solution as described[44]) each, so that each tube contained a series of every sixth section through the sectioned region of the brain. For confocal imaging, sections were immunostained as described previously [44] with the following antibodies (as applicable) at the following respective dilutions: chicken anti-GFP (Aves Labs GFP-1020) 1:1000, guinea pig anti-parvalbumin (Synaptic Systems 195004) 1:1000, sheep anti-tyrosine hydroxylase (Millipore AB1542)) 1:1000, with secondary antibodies donkey anti-chicken Alexa Fluor 488 (Jackson Immuno 703-545-155) 1:200, donkey anti-guinea pig, AlexaFluor 647 conjugated (Jackson Immuno 706-605-148) 1:200, and donkey anti-sheep, AlexaFluor 647 conjugated (Jackson Immuno 713-605-147)) 1:200. Sections were mounted with Prolong Diamond Antifade mounting medium (Thermo Fisher P36970) and imaged on a confocal microscope (Zeiss, LSM 710). For counts, every other series (i.e., either series 1, 3, and 5 or series 2, 4, and 6) of each brain was mounted.

Counts

Neurons labeled with either tdTomato or mCherry in contralateral cortex in PV-Cre mice (crossed with Ai65F reporter mice; see Mouse Strains) and at the injection site in Cre-negative (Ai65F reporter) mice were counted manually by examining every other 50 µm section (i.e., all sections in each of three series, as described in Perfusions and Histology) on an epifluorescence microscope (Zeiss, Imager.Z2).

ACKNOWLEDGEMENTS

We thank Kim Ritola of Janelia Research Campus for helpful discussions regarding the important issue of leaky FLEX viruses as well as Melina Fan and Karen Guerin of Addgene for helpful discussions and for producing the helper AAVs and providing them to our laboratory and to the worldwide neuroscience community. Research reported in this publication was supported by BRAIN Initiative awards U01MH106018, U01MH114829, and U19MH114830 from the National Institute of Mental Health.

REFERENCES CITED

[1] L. Luo, E.M. Callaway, and K. Svoboda, Genetic Dissection of Neural Circuits: A Decade of Progress. Neuron 98 (2018) 865.

[2] K.T. Beier, Hitchhiking on the neuronal highway: Mechanisms of transsynaptic specificity. J Chem Neuroanat 99 (2019) 9-17.

[3] N. Zampieri, T.M. Jessell, and A.J. Murray, Mapping sensory circuits by anterograde transsynaptic transfer of recombinant rabies virus. Neuron 81 (2014) 766-78.

[4] A. Bauer, T. Nolden, J. Schroter, A. Romer-Oberdorfer, S. Gluska, E. Perlson, and S. Finke, Anterograde glycoprotein-dependent transport of newly generated rabies virus in dorsal root ganglion neurons. J Virol 88 (2014) 14172-83.

[5] I.R. Wickersham, D.C. Lyon, R.J. Barnard, T. Mori, S. Finke, K.K. Conzelmann, J.A. Young, and E.M. Callaway, Monosynaptic restriction of transsynaptic tracing from single, genetically targeted neurons. Neuron 53 (2007) 639-47.

[6] I.R. Wickersham, S. Finke, K.K. Conzelmann, and E.M. Callaway, Retrograde neuronal tracing with a deletion-mutant rabies virus. Nature Methods 4 (2007) 47-9.

[7] P. Bates, J.A. Young, and H.E. Varmus, A receptor for subgroup A Rous sarcoma virus is related to the low density lipoprotein receptor. Cell 74 (1993) 1043-51.

[8] J.H. Marshel, T. Mori, K.J. Nielsen, and E.M. Callaway, Targeting single neuronal networks for gene expression and cell labeling in vivo. Neuron 67 (2010) 562-74.

[9] E.A. Rancz, K.M. Franks, M.K. Schwarz, B. Pichler, A.T. Schaefer, and T.W. Margrie, Transfection via whole-cell recording in vivo: bridging single-cell physiology, genetics and connectomics. Nat Neurosci 14 (2011) 527-32.

[10] A. Wertz, S. Trenholm, K. Yonehara, D. Hillier, Z. Raics, M. Leinweber, G. Szalay, A. Ghanem, G. Keller, B. Rozsa, K.K. Conzelmann, and B. Roska, PRESYNAPTIC NETWORKS. Single-cell-initiated monosynaptic tracing reveals layer-specific cortical network modules. Science 349 (2015) 70-4.

[11] S.B. Rompani, F.E. Mullner, A. Wanner, C. Zhang, C.N. Roth, K. Yonehara, and B. Roska, Different Modes of Visual Integration in the Lateral Geniculate Nucleus Revealed by Single-Cell-Initiated Transsynaptic Tracing. Neuron 93 (2017) 1519.

[12] B. Sauer, and N. Henderson, Site-specific DNA recombination in mammalian cells by the Cre recombinase of bacteriophage P1. P Natl Acad Sci USA 85 (1988) 5166-70.
[13] D. Atasoy, Y. Aponte, H.H. Su, and S.M. Sternson, A FLEX switch targets Channelrhodopsin-2 to multiple cell types for imaging and long-range circuit mapping. The Journal of neuroscience : the official journal of the Society for Neuroscience 28 (2008) 7025-30.
[14] N.R. Wall, I.R. Wickersham, A. Cetin, M. De La Parra, and E.M. Callaway, Monosynaptic circuit tracing in vivo through Cre-dependent targeting and complementation of modified rabies virus. Proc Natl Acad Sci U S A 107 (2010) 21848-53.
[15] M. Watabe-Uchida, L. Zhu, S.K. Ogawa, A. Vamanrao, and N. Uchida, Whole-brain mapping of direct inputs to midbrain dopamine neurons. Neuron 74 (2012) 858-73.
[16] K. Kohara, M. Pignatelli, A.J. Rivest, H.Y. Jung, T. Kitamura, J. Suh, D. Frank, K. Kajikawa, N. Mise, Y. Obata, I.R. Wickersham, and S. Tonegawa, Cell type-specific genetic and optogenetic tools reveal hippocampal CA2 circuits. Nat Neurosci 17 (2014) 269-79.
[17] K.T. Beier, E.E. Steinberg, K.E. DeLoach, S. Xie, K. Miyamichi, L. Schwarz, X.J. Gao, E.J. Kremer, R.C. Malenka, and L. Luo, Circuit Architecture of VTA Dopamine Neurons Revealed by Systematic Input-Output Mapping. Cell 162 (2015) 622-34.
[18] K. Liu, J. Kim, D.W. Kim, Y.S. Zhang, H. Bao, M. Denaxa, S.A. Lim, E. Kim, C. Liu, I.R. Wickersham, V. Pachinis, S. Hattar, J. Song, S.P. Brown, and S. Blackshaw, Lhx6-positive GABA-releasing neurons of the zona incerta promote sleep. Nature 548 (2017) 582-587.
[19] S. Ahrlund-Richter, Y. Xuan, J.A. van Lunteren, H. Kim, C. Ortiz, I. Pollak Dorocic, K. Meletis, and M. Carlen, A whole-brain atlas of monosynaptic input targeting four different cell types in the medial prefrontal cortex of the mouse. Nat Neurosci 22 (2019) 657-668.
[20] Z. Zhang, P. Zhong, F. Hu, Z. Barger, Y. Ren, X. Ding, S. Li, F. Weber, S. Chung, R.D. Palmiter, and Y. Dan, An Excitatory Circuit in the Perioculomotor Midbrain for Non-REM Sleep Control. Cell 177 (2019) 1293-1307 e16.
[21] A. Szonyi, K.E. Sos, R. Nyilas, D. Schlingloff, A. Domonkos, V.T. Takacs, B. Posfai, P. Hegedus, J.B. Priestley, A.L. Gundlach, A.I. Gulyas, V. Varga, A. Losonczy, T.F. Freund, and G. Nyiri, Brainstem nucleus incertus controls contextual memory formation. Science 364 (2019).
[22] M.J. Federspiel, P. Bates, J.A. Young, H.E. Varmus, and S.H. Hughes, A system for tissue-specific gene targeting: transgenic mice susceptible to subgroup A avian leukosis virus-based retroviral vectors. Proc Natl Acad Sci U S A 91 (1994) 11241-5.
[23] B. Seidler, A. Schmidt, U. Mayr, H. Nakhai, R.M. Schmid, G. Schneider, and D. Saur, A Cre-loxP-based mouse model for conditional somatic gene expression and knockdown in vivo by using avian retroviral vectors. Proc Natl Acad Sci U S A 105 (2008) 10137-42.
[24] K. Miyamichi, Y. Shlomai-Fuchs, M. Shu, B.C. Weissbourd, L. Luo, and A. Mizrahi, Dissecting local circuits: parvalbumin interneurons underlie broad feedback control of olfactory bulb output. Neuron 80 (2013) 1232-45.
[25] K. Sakurai, S. Zhao, J. Takatoh, E. Rodriguez, J. Lu, A.D. Leavitt, M. Fu, B.X. Han, and F. Wang, Capturing and Manipulating Activated Neuronal Ensembles with CANE Delineates a Hypothalamic Social-Fear Circuit. Neuron 92 (2016) 739-753.
[26] M. Gossen, and H. Bujard, Tight control of gene expression in mammalian cells by tetracycline-responsive promoters. Proc Natl Acad Sci U S A 89 (1992) 5547-51.
[27] J.A. Young, P. Bates, and H.E. Varmus, Isolation of a chicken gene that confers susceptibility to infection by subgroup A avian leukosis and sarcoma viruses. J Virol 67 (1993) 1811-6.
[28] N.K. Jha, O. Latinovic, E. Martin, G. Novitskiy, M. Marin, K. Miyauchi, J. Naughton, J.A. Young, and G.B. Melikyan, Imaging single retrovirus entry through alternative receptor isoforms and intermediates of virus-endosome fusion. PLoS Pathog 7 (2011) e1001260.
[29] B.P. Cormack, R.H. Valdivia, and S. Falkow, FACS-optimized mutants of the green fluorescent protein (GFP). Gene 173 (1996) 33-8.
[30] K.K. Conzelmann, J.H. Cox, L.G. Schneider, and H.J. Thiel, Molecular cloning and complete nucleotide sequence of the attenuated rabies virus SAD B19. Virology 175 (1990) 485-99.
[31] O.M. Subach, P.J. Cranfill, M.W. Davidson, and V.V. Verkhusha, An enhanced monomeric blue fluorescent protein with the high chemical stability of the chromophore. PLoS One 6 (2011) e28674.
[32] S. Hippenmeyer, E. Vrieseling, M. Sigrist, T. Portmann, C. Laengle, D.R. Ladle, and S. Arber, A developmental switch in the response of DRG neurons to ETS transcription factor signaling. PLoS Biol 3 (2005) e159.

[33] N.C. Shaner, R.E. Campbell, P.A. Steinbach, B.N. Giepmans, A.E. Palmer, and R.Y. Tsien, Improved monomeric red, orange and yellow fluorescent proteins derived from Discosoma sp. red fluorescent protein. Nat Biotechnol 22 (2004) 1567-72.
[34] T.L. Daigle, L. Madisen, T.A. Hage, M.T. Valley, U. Knoblich, R.S. Larsen, M.M. Takeno, L. Huang, H. Gu, R. Larsen, M. Mills, A. Bosma-Moody, L.A. Siverts, M. Walker, L.T. Graybuck, Z. Yao, O. Fong, T.N. Nguyen, E. Garren, G.H. Lenz, M. Chavarha, J. Pendergraft, J. Harrington, K.E. Hirokawa, J.A. Harris, P.R. Nicovich, M.J. McGraw, D.R. Ollerenshaw, K.A. Smith, C.A. Baker, J.T. Ting, S.M. Sunkin, J. Lecoq, M.Z. Lin, E.S. Boyden, G.J. Murphy, N.M. da Costa, J. Waters, L. Li, B. Tasic, and H. Zeng, A Suite of Transgenic Driver and Reporter Mouse Lines with Enhanced Brain-Cell-Type Targeting and Functionality. Cell 174 (2018) 465-480 e22.
[35] C.S. Raymond, and P. Soriano, High-efficiency FLP and PhiC31 site-specific recombination in mammalian cells. PLoS One 2 (2007) e162.
[36] C.M. Backman, N. Malik, Y. Zhang, L. Shan, A. Grinberg, B.J. Hoffer, H. Westphal, and A.C. Tomac, Characterization of a mouse strain expressing Cre recombinase from the 3' untranslated region of the dopamine transporter locus. Genesis 44 (2006) 383-90.
[37] A.P. Weible, L. Schwarcz, I.R. Wickersham, L. Deblander, H. Wu, E.M. Callaway, H.S. Seung, and C.G. Kentros, Transgenic targeting of recombinant rabies virus reveals monosynaptic connectivity of specific neurons. The Journal of neuroscience : the official journal of the Society for Neuroscience 30 (2010) 16509-13.
[38] I.R. Wickersham, H.A. Sullivan, and H.S. Seung, Production of glycoprotein-deleted rabies viruses for monosynaptic tracing and high-level gene expression in neurons. Nature protocols 5 (2010) 595-606.
[39] I.R. Wickersham, and H.A. Sullivan, Rabies viral vectors for monosynaptic tracing and targeted transgene expression in neurons. Cold Spring Harb Protoc 2015 (2015) 375-85.
[40] S. Chatterjee, H.A. Sullivan, B.J. MacLennan, R. Xu, Y. Hou, T.K. Lavin, N.E. Lea, J.E. Michalski, K.R. Babcock, S. Dietrich, G.A. Matthews, A. Beyeler, G.G. Calhoon, G. Glober, J.D. Whitesell, S. Yao, A. Cetin, J.A. Harris, H. Zeng, K.M. Tye, R.C. Reid, and I.R. Wickersham, Nontoxic, double-deletion-mutant rabies viral vectors for retrograde targeting of projection neurons. Nat Neurosci 21 (2018) 638-646.
[41] L. Madisen, A.R. Garner, D. Shimaoka, A.S. Chuong, N.C. Klapoetke, L. Li, A. van der Bourg, Y. Niino, L. Egolf, C. Monetti, H. Gu, M. Mills, A. Cheng, B. Tasic, T.N. Nguyen, S.M. Sunkin, A. Benucci, A. Nagy, A. Miyawaki, F. Helmchen, R.M. Empson, T. Knopfel, E.S. Boyden, R.C. Reid, M. Carandini, and H. Zeng, Transgenic mice for intersectional targeting of neural sensors and effectors with high specificity and performance. Neuron 85 (2015) 942-58.
[42] M.D. Tallquist, and P. Soriano, Epiblast-restricted Cre expression in MORE mice: a tool to distinguish embryonic vs. extra-embryonic gene function. Genesis 26 (2000) 113-5.
[43] L. Madisen, T.A. Zwingman, S.M. Sunkin, S.W. Oh, H.A. Zariwala, H. Gu, L.L. Ng, R.D. Palmiter, M.J. Hawrylycz, A.R. Jones, E.S. Lein, and H. Zeng, A robust and high-throughput Cre reporting and characterization system for the whole mouse brain. Nature neuroscience 13 (2010) 133-40.
[44] T.K. Lavin, L. Jin and I. Wickersham, Monosynaptic tracing: A step-by-step protocol. J of chemical anatomy (2019). https://doi.org/10.1016/j.jchemneu.2019.101661.
[45] M. Matsuyama, L. Jin, T.K. Lavin, H.A. Sullivan, Y. Hou, N.E. Lea, M.T. Pruner, M.L. Dam Ferdínez, and I.R. Wickersham, "Self-inactivating" rabies viruses are just first-generation, ΔG rabies viruses. bioRxiv (2019) https://doi.org/10.1101/550640.

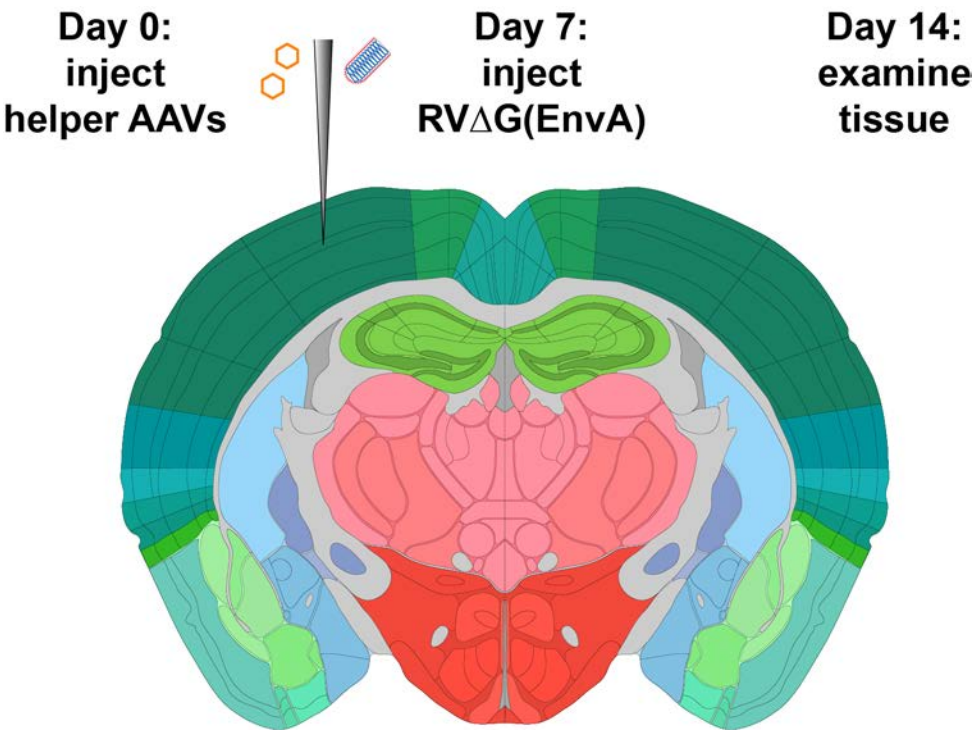

Figure 1: Strategy for monosynaptic tracing with helper AAVs. Helper viruses are injected in a Cre mouse, or a Cre-negative mouse in the case of control experiments, then rabies virus (RV) (∆G, EnvA-coated, expressing mCherry) is injected in the same location subsequently. While different labs have used various intervals and survival times, we used a 7-day interval between AAV and RV injections, and another 7-day interval between RV injection and perfusion, in all experiments for this paper.

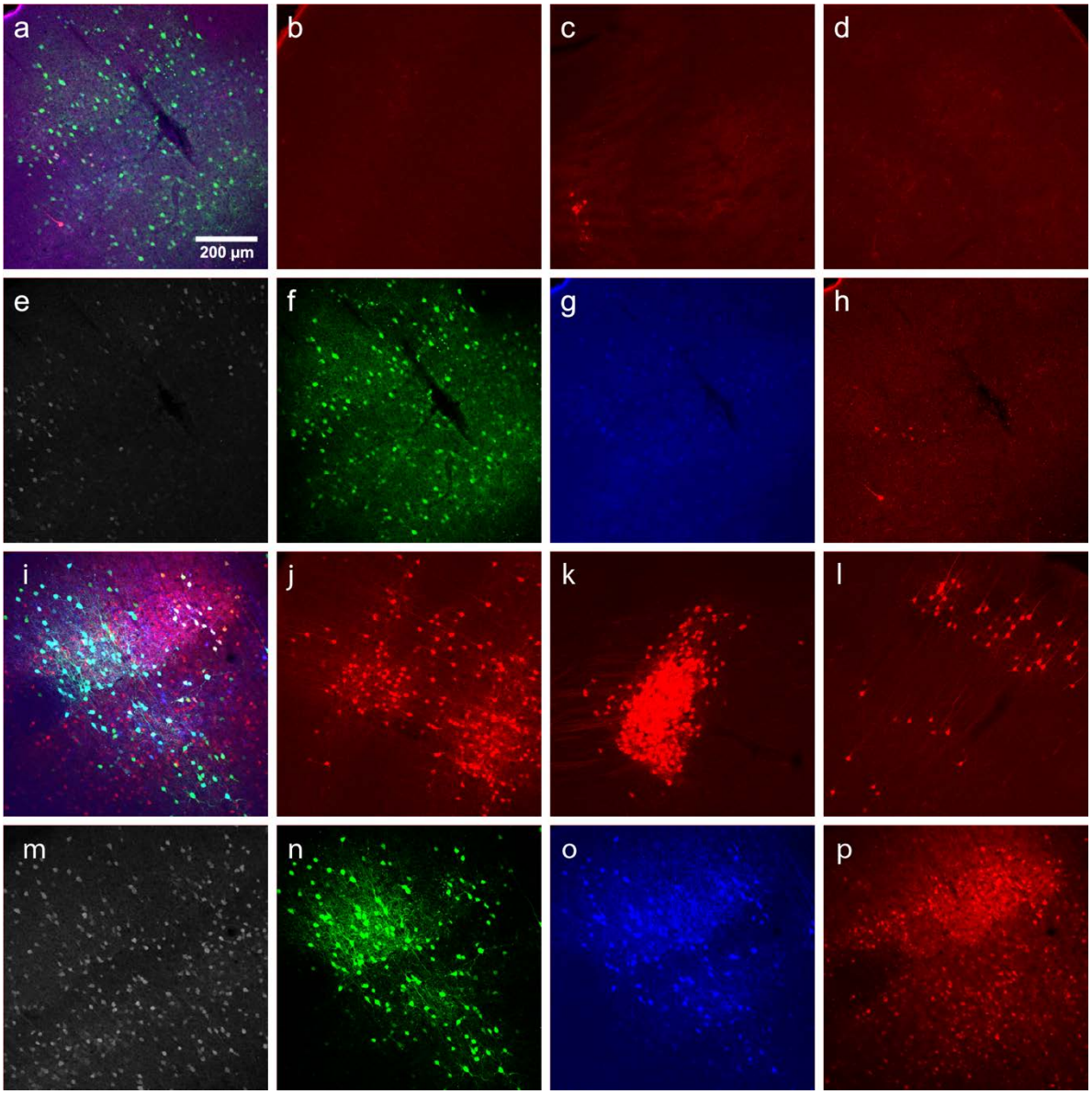

Figure 2: Use of helper viruses at excessive concentrations can result in near-complete failure of monosynaptic tracing. The two-AAV combination described in Liu et al.[18] (AAV1-synP-FLEX-splitTVA-EGFP-B19G mixed with AAV1-TREtight-mTagBFP2-B19G) was injected in somatosensory cortex of PV-Cre x Ai65F (FLPo-dependent tdTomato reporter) mice, followed by RVΔG-4FLPo(EnvA) 7 days later. a-h) Very poor results were obtained when using new preparations of these AAVs undiluted. a) Injection site in S1. Green = anti-EGFP staining, blue = mTagBFP2, red = tdTomato. Individual channels from this field are shown in panels e-h. b) No labeled neurons were found in ipsilateral secondary somatosensory cortex. c) Very few labeled neurons were found in ipsilateral thalamus (VPM and Po). d) No labeled neurons were found in contralateral S1. e-h) Individual channels from the field shown in panel a. e) anti-parvalbumin staining (not shown in panel a). f) anti-EGFP staining, indicating expression from the first, Cre-dependent AAV. g) mTagBFP2, indicating expression from the second, tTA-dependent AAV. h) tdTomato, reporting activity of the FLPo-encoding rabies virus. i-p) Diluting the helper viruses to concentrations matching previously used preparations gave much better results. i) Injection site in S1; individual channels from this field are shown in panels m-p. j-l) Many labeled presynaptic neurons were found in ipsilateral secondary somatosensory cortex (j), ipsilateral thalamus (VPM and Po) (k), and contralateral S1 (l). m) anti-parvalbumin staining (not shown in panel a). n) anti-EGFP staining, indicating expression from the first, Cre-dependent AAV. o) mTagBFP2, indicating expression from the second, G-encoding AAV. p) tdTomato, reporting activity of the FLPo-encoding rabies virus. Scale bar in a: 200 µm, applies to all panels.

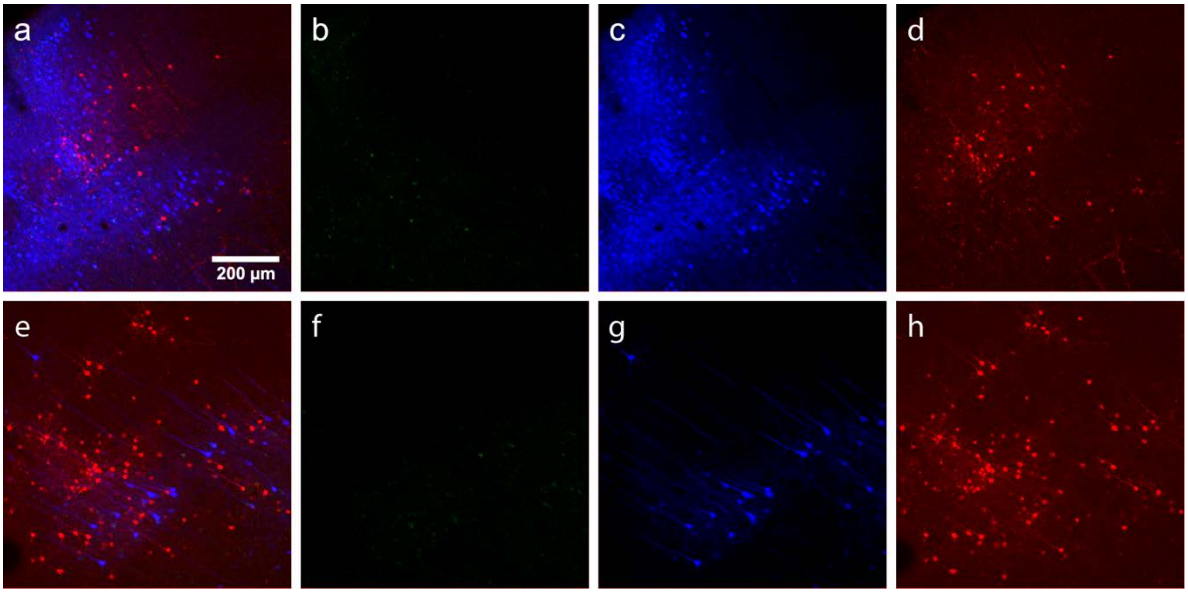

Figure 3: Use of insufficiently-diluted helper viruses results in excessive background labeling in Cre-negative animals. a-d) Injection site after using undiluted viruses in two-helper combination: many labeled cells are seen. a) Overlay of b-d. b) anti-EGFP staining, c) mTagBFP2 signal, d) tdTomato marking RV labeling. e-h) Even with the AAVs diluted to match the titers of previous batches, excessive background labeling is seen at the injection site. e) Overlay of f-h. f) anti-EGFP staining, g) mTagBFP2 signal, h) tdTomato marking RV labeling. Scale bar in a: 200 µm, applies to all panels.

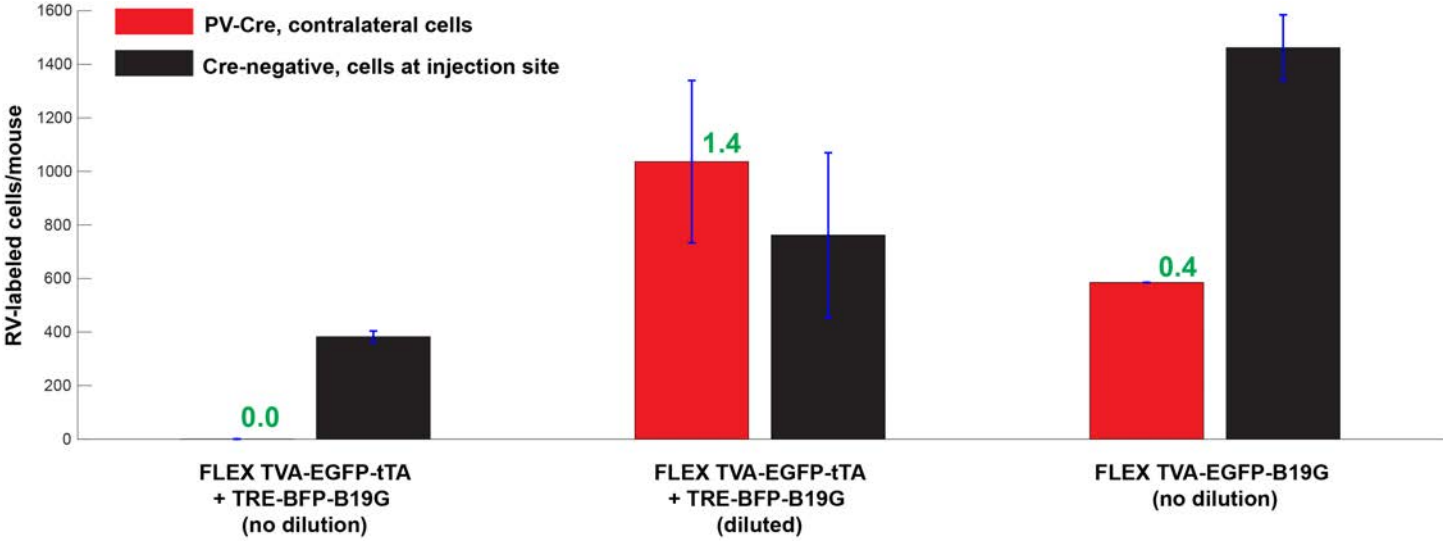

Figure 4: Quantification of results in PV-Cre and Cre-negative mice: pilot study with helper viruses either undiluted or diluted to titers used in previous work. Red depicts numbers of neurons labeled by RV in contralateral cortex (in every other 50 µm section) in PV-Cre mice; black depicts numbers of RV-labeled neurons in the vicinity of the injection site, i.e. in ipsilateral cortex (in every other 50 µm section) in Cre-negative mice. Numbers in green represent the ratio of contralateral neurons in Cre+ mice to ipsilateral neurons in Cre- mice. "Diluted" here means diluted to the titers of other batches used previously in our laboratory; see main text for details. Excessive concentrations of helper viruses gave very poor results. Source numbers are provided in table S1.

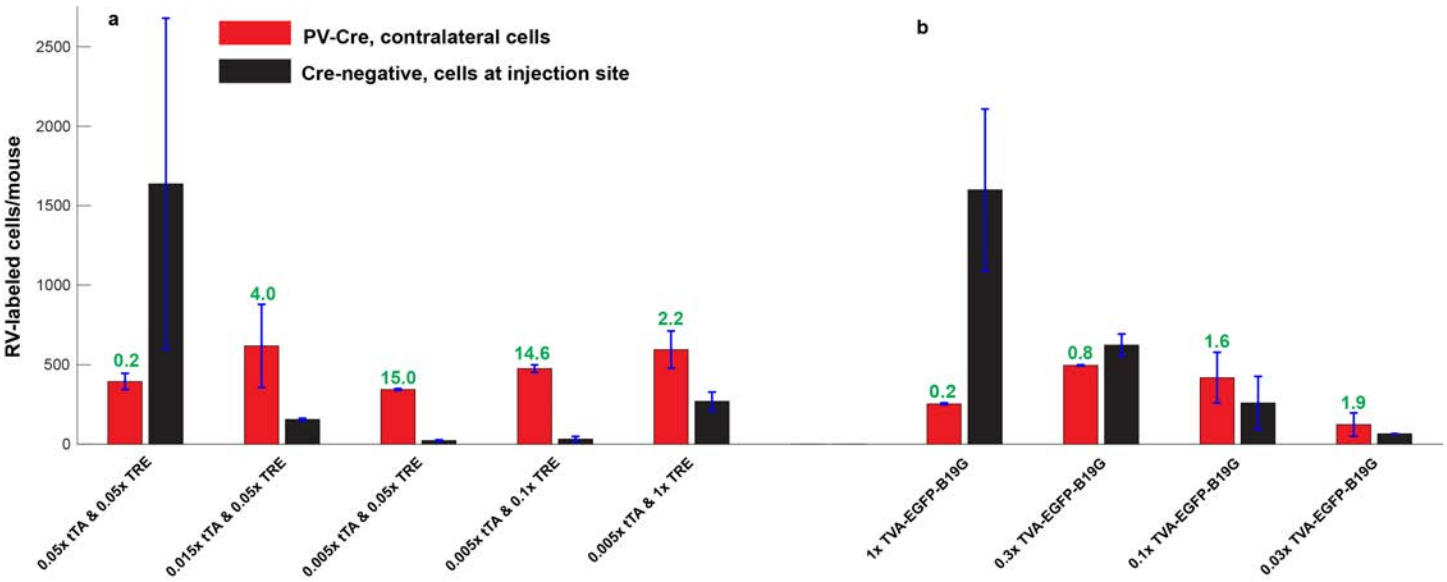

Figure 5: Quantification of results in PV-Cre and Cre-negative mice: systematic dilution series. a) Results of varying the concentrations of the two helper viruses in the tTA-TRE combination system. The highest ratio of contralateral neurons in Cre+ mice to ipsilateral neurons in Cre- mice was obtained with a 1:200 dilution of AAV1-syn-FLEX-splitTVA-EGFP-tTA and a 1:20 dilution of AAV1-TREtight-mTagBFP2-B19G ("0.005x tTA & 0.05x TRE" in the figure). b) Results of varying the concentration of the single helper virus AAV1-syn-FLEX-splitTVA-EGFP-B19G. Higher dilutions (out to 1:33.3) give higher ratios of contralateral neurons in Cre+ mice to ipsilateral neurons in Cre- mice, but results with the single-helper approach were nowhere near as good as with the two-helper combination. Source numbers are provided in table S1.

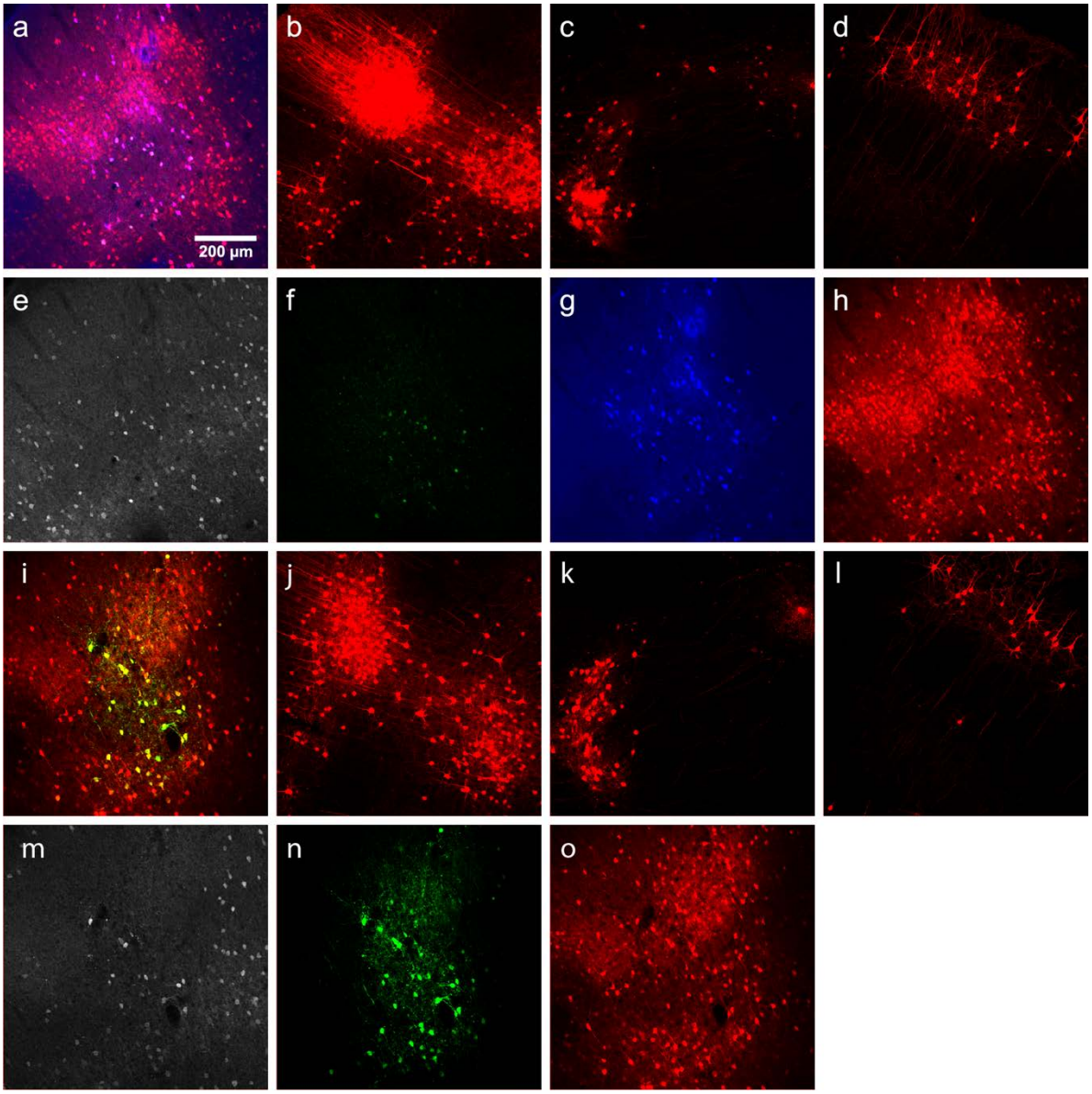

Figure 6: Example results using recommended dilutions of helper viruses in PV-Cre mice. a-h) Use of the two-AAV combination at 1:200 and 1:20 dilutions (see main text) labeled many presynaptic neurons. a) Injection site in S1. Green = anti-EGFP staining, blue = mTagBFP2, red = mCherry. Individual channels from this field are shown in panels e-h. b) Many labeled neurons were found in ipsilateral S2. c) Many labeled neurons were found in ipsilateral thalamus (VPM and Po). d) Many labeled neurons were found in contralateral S1. e-h) Individual channels from the field shown in panel a. e) anti-parvalbumin staining (not shown in panel a). f) anti-EGFP staining, indicating expression from the first, Cre-dependent AAV. Note that, at this dilution, EGFP signal is quite dim even with immunoamplification. g) mTagBFP2, indicating expression from the second, tTA-dependent AAV. h) mCherry, indicating presence of the ΔG rabies virus. i-o) Use of the single tricistronic helper AAV at 1:10 dilution (see main text) also labeled many presynaptic neurons (but see Figure 7). i) Injection site in S1; individual channels from this field are shown in panels m-o. j) Labeled neurons in ipsilateral S2. k) Labeled neurons in ipsilateral thalamus (VPM and Po). l) Labeled neurons in contralateral S1. m) anti-parvalbumin staining (not shown in panel i). n) anti-EGFP staining, indicating expression from the first, Cre-dependent AAV. o) mCherry, indicating presence of the ΔG rabies virus. Scale bar in a: 200 µm, applies to all panels.

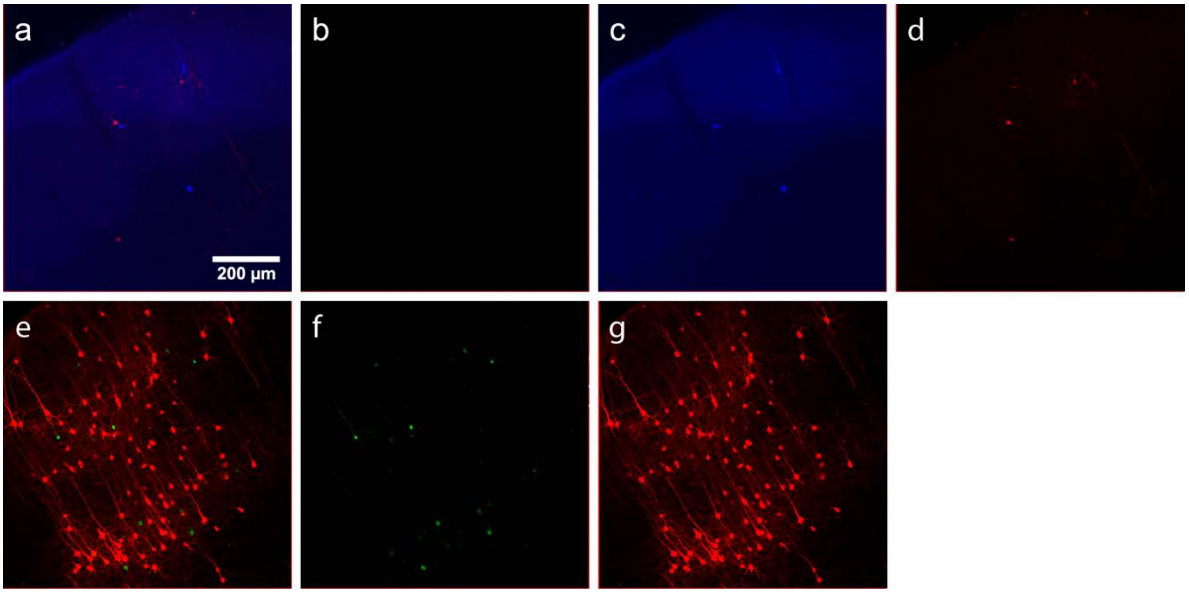

Figure 7: Results using recommended dilutions of helper viruses in Cre-negative mice. a-d) Injection site after using two-helper combination at 1:200 & 1:20 (see main text): few mCherry-labeled cells are seen. a) Overlay of b-d. b) anti-EGFP staining: no signal is visible, even with amplification. c) mTagBFP2 signal. A few blue cells are seen even at these dilutions. d) mCherry expressed by RV. e-g) Injection site after using single tricistronic helper: many mCherry-labeled neurons are present. e) Overlay of f-g. f) anti-EGFP staining: significant signal is seen even in these Cre-negative mice. g) mCherry expressed by RV. Scale bar in a: 200 µm, applies to all panels.

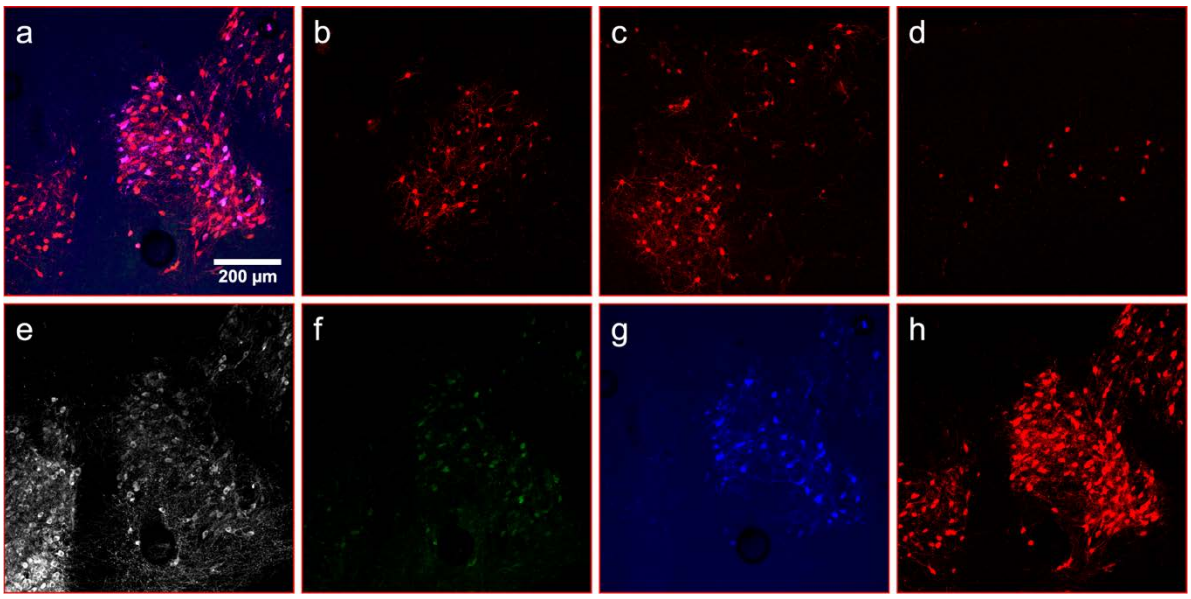

Figure 8: Inputs to dopaminergic cells in DAT-Cre, using recommended dilutions of two-helper combination. a) Injection site in VTA/SNc: overlay of panels f-h. b) RV-labeled cells in dorsal striatum. c) RV-labeled cells in ventral striatum. d) RV-labeled cells in cortex. e) anti-tyrosine hydroxylase (TH) staining (not shown in panel a). f) anti-EGFP staining, indicating expression from the first, Cre-dependent AAV. g) mTagBFP2, indicating expression from the second, tTA-dependent AAV. h) tdTomato, reporting activity of the FLPo-encoding rabies virus. Scale bar in a: 200 µm, applies to all panels.

Table S1: Counts of labeled cells in PV-Cre and Cre-negative mice. Numbers of labeled neurons in contralateral cortex of PV-Cre mice and at the injection site of Cre-negative mice for the various helper virus conditions. Each number in the "# cells" column indicates the total number of labeled cells found in the examined region (either the vicinity of the injection site or the contralateral cortex) across all 50 μm sections in that series of every sixth section (see methods). The total number of labeled neurons counted for a given mouse was the sum of the total labeled neurons in each of the three examined series for that mouse (i.e., the total found in every other section). The means and SEMs of the total numbers of labeled neurons for each condition are graphed in Figures 4 and 5.

virus condition	genotype	mouse #	series #	count location	# cells	notes
PILOT EXPERIMENTS WITH RVΔG-4FLPo						
sTpEptTA (undiluted)	PV-Cre	18022606NL	1	Contralateral Cortex	0	
sTpEptTA (undiluted)	PV-Cre	18022606NL	3	Contralateral Cortex	0	
sTpEptTA (undiluted)	PV-Cre	18022606NL	5	Contralateral Cortex	1	
sTpEptTA (undiluted)	PV-Cre	18022606LJ	1	Contralateral Cortex	0	
sTpEptTA (undiluted)	PV-Cre	18022606LJ	3	Contralateral Cortex	0	
sTpEptTA (undiluted)	PV-Cre	18022606LJ	5	Contralateral Cortex	0	
sTpEptTA (undiluted)	Cre-negative	18030501LJ	1	Injection Site	124	
sTpEptTA (undiluted)	Cre-negative	18030501LJ	3	Injection Site	140	
sTpEptTA (undiluted)	Cre-negative	18030501LJ	5	Injection Site	140	
sTpEptTA (undiluted)	Cre-negative	18030502LJ	1	Injection Site	120	
sTpEptTA (undiluted)	Cre-negative	18030502LJ	3	Injection Site	112	
sTpEptTA (undiluted)	Cre-negative	18030502LJ	5	Injection Site	129	
sTpEptTA (diluted)	PV-Cre	18050701LJ	2	Contralateral Cortex	247	
sTpEptTA (diluted)	PV-Cre	18050701LJ	4	Contralateral Cortex	240	
sTpEptTA (diluted)	PV-Cre	18050701LJ	6	Contralateral Cortex	246	
sTpEptTA (diluted)	PV-Cre	18050702TL	2	Contralateral Cortex	475	
sTpEptTA (diluted)	PV-Cre	18050702TL	4	Contralateral Cortex	422	
sTpEptTA (diluted)	PV-Cre	18050702TL	6	Contralateral Cortex	443	
sTpEptTA (diluted)	Cre-negative	18050702LJ	2	Injection Site	363	
sTpEptTA (diluted)	Cre-negative	18050702LJ	4	Injection Site	374	
sTpEptTA (diluted)	Cre-negative	18050702LJ	6	Injection Site	333	
sTpEptTA (diluted)	Cre-negative	18050701TL	2	Injection Site	151	
sTpEptTA (diluted)	Cre-negative	18050701TL	4	Injection Site	156	
sTpEptTA (diluted)	Cre-negative	18050701TL	6	Injection Site	147	
sTpEpB (undiluted)	PV-Cre	18022605LJ	1	Contralateral Cortex	201	
sTpEpB (undiluted)	PV-Cre	18022605LJ	3	Contralateral Cortex	180	
sTpEpB (undiluted)	PV-Cre	18022605LJ	5	Contralateral Cortex	204	

sTpEpB (undiluted)	PV-Cre	18030101LJ	1	Contralateral Cortex	0	poor perfusion
sTpEpB (undiluted)	PV-Cre	18030101LJ	3	Contralateral Cortex	0	poor perfusion
sTpEpB (undiluted)	PV-Cre	18030101LJ	5	Contralateral Cortex	0	poor perfusion
sTpEpB (undiluted)	Cre-negative	18030102LJ	1	Injection Site	531	
sTpEpB (undiluted)	Cre-negative	18030102LJ	3	Injection Site	541	
sTpEpB (undiluted)	Cre-negative	18030102LJ	5	Injection Site	513	
sTpEpB (undiluted)	Cre-negative	18030103LJ	1	Injection Site	499	
sTpEpB (undiluted)	Cre-negative	18030103LJ	3	Injection Site	433	
sTpEpB (undiluted)	Cre-negative	18030103LJ	5	Injection Site	408	

SYSTEMATIC DILUTION SERIES: SINGLE TRICISTRONIC HELPER

1x sTpEpB	PV-Cre	18052302LJ	2	Contralateral cortex	76	
1x sTpEpB	PV-Cre	18052302LJ	4	Contralateral cortex	97	
1x sTpEpB	PV-Cre	18052302LJ	6	Contralateral cortex	87	
1x sTpEpB	PV-Cre	18052302TL	2	Contralateral cortex	83	
1x sTpEpB	PV-Cre	18052302TL	4	Contralateral cortex	78	
1x sTpEpB	PV-Cre	18052302TL	6	Contralateral cortex	87	
1x sTpEpB	Cre-negative	18052301LJ	2	injection site	339	
1x sTpEpB	Cre-negative	18052301LJ	4	injection site	347	
1x sTpEpB	Cre-negative	18052301LJ	6	injection site	405	
1x sTpEpB	Cre-negative	18052301TL	2	injection site	716	
1x sTpEpB	Cre-negative	18052301TL	4	injection site	729	
1x sTpEpB	Cre-negative	18052301TL	6	injection site	663	

0.3x sTpEpB	PV-Cre	18052304LJ	2	Contralateral cortex	186	
0.3x sTpEpB	PV-Cre	18052304LJ	4	Contralateral cortex	139	
0.3x sTpEpB	PV-Cre	18052304LJ	6	Contralateral cortex	175	
0.3x sTpEpB	PV-Cre	18052304TL	2	Contralateral cortex	161	
0.3x sTpEpB	PV-Cre	18052304TL	4	Contralateral cortex	161	
0.3x sTpEpB	PV-Cre	18052304TL	6	Contralateral cortex	170	
0.3x sTpEpB	Cre-negative	18052303LJ	2	injection site	184	
0.3x sTpEpB	Cre-negative	18052303LJ	4	injection site	183	

0.3x sTpEpB	Cre-negative	18052303LJ	6	injection site	187	
0.3x sTpEpB	Cre-negative	18052303TL	2	injection site	226	
0.3x sTpEpB	Cre-negative	18052303TL	4	injection site	252	
0.3x sTpEpB	Cre-negative	18052303TL	6	injection site	215	
0.1x sTpEpB	PV-Cre	18052502LJ	1	Contralateral cortex	77	
0.1x sTpEpB	PV-Cre	18052502LJ	3	Contralateral cortex	79	
0.1x sTpEpB	PV-Cre	18052502LJ	5	Contralateral cortex	103	
0.1x sTpEpB	PV-Cre	18052502TL	1	Contralateral cortex	246	
0.1x sTpEpB	PV-Cre	18052502TL	3	Contralateral cortex	249	
0.1x sTpEpB	PV-Cre	18052502TL	5	Contralateral cortex	83	
0.1x sTpEpB	Cre-negative	18052501TL	1	injection site	28	
0.1x sTpEpB	Cre-negative	18052501TL	3	injection site	36	
0.1x sTpEpB	Cre-negative	18052501TL	5	injection site	29	
0.1x sTpEpB	Cre-negative	18052501LJ	1	injection site	113	
0.1x sTpEpB	Cre-negative	18052501LJ	3	injection site	170	
0.1x sTpEpB	Cre-negative	18052501LJ	5	injection site	143	
0.03x sTpEpB	PV-Cre	18091801NL	2	Contralateral cortex	13	
0.03x sTpEpB	PV-Cre	18091801NL	4	Contralateral cortex	17	
0.03x sTpEpB	PV-Cre	18091801NL	6	Contralateral cortex	20	
0.03x sTpEpB	PV-Cre	18091802NL	2	Contralateral cortex	69	
0.03x sTpEpB	PV-Cre	18091802NL	4	Contralateral cortex	57	
0.03x sTpEpB	PV-Cre	18091802NL	6	Contralateral cortex	71	
0.03x sTpEpB	Cre-negative	18091804NL	2	injection site	18	
0.03x sTpEpB	Cre-negative	18091804NL	4	injection site	28	
0.03x sTpEpB	Cre-negative	18091804NL	6	injection site	20	

SYSTEMATIC DILUTION SERIES: TWO-HELPER COMBINATION

0.05x tTA & 0.05x TRE	PV-Cre	18052402LJ	2	Contralateral Cortex	124	damaged
0.05x tTA & 0.05x TRE	PV-Cre	18052402LJ	4	Contralateral Cortex	97	damaged
0.05x tTA & 0.05x TRE	PV-Cre	18052402LJ	6	Contralateral Cortex	122	damaged

0.05x tTA & 0.05x TRE	PV-Cre	18052402TL	2	Contralateral Cortex	150	
0.05x tTA & 0.05x TRE	PV-Cre	18052402TL	4	Contralateral Cortex	145	
0.05x tTA & 0.05x TRE	PV-Cre	18052402TL	6	Contralateral Cortex	151	
0.05x tTA & 0.05x TRE	Cre-negative	18052401LJ	2	Injection Site	411	
0.05x tTA & 0.05x TRE	Cre-negative	18052401LJ	4	Injection Site	443	
0.05x tTA & 0.05x TRE	Cre-negative	18052401LJ	6	Injection Site	1825	
0.05x tTA & 0.05x TRE	Cre-negative	18052401TL	2	Injection Site	220	
0.05x tTA & 0.05x TRE	Cre-negative	18052401TL	4	Injection Site	186	
0.05x tTA & 0.05x TRE	Cre-negative	18052401TL	6	Injection Site	191	
0.015x tTA & 0.05x TRE	PV-Cre	18052404LJ	2	Contralateral Cortex	114	
0.015x tTA & 0.05x TRE	PV-Cre	18052404LJ	4	Contralateral Cortex	130	
0.015x tTA & 0.05x TRE	PV-Cre	18052404LJ	6	Contralateral Cortex	113	
0.015x tTA & 0.05x TRE	PV-Cre	18052404TL	2	Contralateral Cortex	289	
0.015x tTA & 0.05x TRE	PV-Cre	18052404TL	4	Contralateral Cortex	303	
0.015x tTA & 0.05x TRE	PV-Cre	18052404TL	6	Contralateral Cortex	287	
0.015x tTA & 0.05x TRE	Cre-negative	18052403LJ	2	Injection Site	52	
0.015x tTA & 0.05x TRE	Cre-negative	18052403LJ	4	Injection Site	48	
0.015x tTA & 0.05x TRE	Cre-negative	18052403LJ	6	Injection Site	48	
0.015x tTA & 0.05x TRE	Cre-negative	18052403TL	2	Injection Site	57	
0.015x tTA & 0.05x TRE	Cre-negative	18052403TL	4	Injection Site	41	
0.015x tTA & 0.05x TRE	Cre-negative	18052403TL	6	Injection Site	65	
0.005x tTA & 0.05x TRE	PV-Cre	18052406LJ	1	Contralateral cortex	122	
0.005x tTA & 0.05x TRE	PV-Cre	18052406LJ	3	Contralateral cortex	127	
0.005x tTA & 0.05x TRE	PV-Cre	18052406LJ	5	Contralateral cortex	101	
0.005x tTA & 0.05x TRE	PV-Cre	18052406TL	1	Contralateral cortex	114	
0.005x tTA & 0.05x TRE	PV-Cre	18052406TL	3	Contralateral cortex	124	
0.005x tTA & 0.05x TRE	PV-Cre	18052406TL	5	Contralateral cortex	100	
0.005x tTA & 0.05x TRE	Cre-negative	18052405LJ	1	injection site	9	
0.005x tTA & 0.05x TRE	Cre-negative	18052405LJ	3	injection site	1	
0.005x tTA & 0.05x TRE	Cre-negative	18052405LJ	5	injection site	8	
0.005x tTA & 0.05x TRE	Cre-negative	18052405TL	1	injection site	10	

0.005x tTA & 0.05x TRE	Cre-negative	18052405TL	3	injection site	7	
0.005x tTA & 0.05x TRE	Cre-negative	18052405TL	5	injection site	11	
0.005x tTA & 0.1x TRE	PV-Cre	18092101NL	2	Contralateral cortex	163	
0.005x tTA & 0.1x TRE	PV-Cre	18092101NL	4	Contralateral cortex	171	
0.005x tTA & 0.1x TRE	PV-Cre	18092101NL	6	Contralateral cortex	165	
0.005x tTA & 0.1x TRE	PV-Cre	18092102NL	2	Contralateral cortex	150	
0.005x tTA & 0.1x TRE	PV-Cre	18092102NL	4	Contralateral cortex	146	
0.005x tTA & 0.1x TRE	PV-Cre	18092102NL	6	Contralateral cortex	156	
0.005x tTA & 0.1x TRE	Cre-negative	18092103NL	2	injection site	13	
0.005x tTA & 0.1x TRE	Cre-negative	18092103NL	4	injection site	14	
0.005x tTA & 0.1x TRE	Cre-negative	18092103NL	6	injection site	22	
0.005x tTA & 0.1x TRE	Cre-negative	18092104NL	2	injection site	4	
0.005x tTA & 0.1x TRE	Cre-negative	18092104NL	4	injection site	7	
0.005x tTA & 0.1x TRE	Cre-negative	18092104NL	6	injection site	5	
0.005x tTA & 1x TRE	PV-Cre	18091901NL	2	Contralateral cortex	191	
0.005x tTA & 1x TRE	PV-Cre	18091901NL	4	Contralateral cortex	137	
0.005x tTA & 1x TRE	PV-Cre	18091901NL	6	Contralateral cortex	149	
0.005x tTA & 1x TRE	PV-Cre	18091902NL	2	Contralateral cortex	260	
0.005x tTA & 1x TRE	PV-Cre	18091902NL	4	Contralateral cortex	236	
0.005x tTA & 1x TRE	PV-Cre	18091902NL	6	Contralateral cortex	216	
0.005x tTA & 1x TRE	Cre-negative	18092001NL	2	injection site	58	
0.005x tTA & 1x TRE	Cre-negative	18092001NL	4	injection site	89	
0.005x tTA & 1x TRE	Cre-negative	18092001NL	6	injection site	65	
0.005x tTA & 1x TRE	Cre-negative	18092002NL	2	injection site	130	
0.005x tTA & 1x TRE	Cre-negative	18092002NL	4	injection site	106	
0.005x tTA & 1x TRE	Cre-negative	18092002NL	6	injection site	92	